Multiscale machinability analysis of natural fiber composites

1. **Faissal Chegdani** *

   - Arts et Metiers Institute of Technology, MSMP, HESAM Université, F-51006, Châlons-en-Champagne, France.

   Email: faissal.chegdani@ensam.eu

2. **Mohamed El Mansori**

   - Arts et Metiers Institute of Technology, MSMP, HESAM Université, F-51006, Châlons-en-Champagne, France
   - Texas A&M Engineering Experiment Station, Institute for Manufacturing Systems, College Station, TX 77843, USA

   Email: mohamed.elmansori@ensam.eu

ABSTRACT: (50-100 words)

Machinability qualification of natural fiber composites requires a specific approach that involves the multiscale structure of natural fibers. This chapter addresses the machining qualification issues for natural fiber composites and proposes a new multiscale approach to analyze the topography of the machined surfaces. Results show that machining of natural fiber composites requires specific analysis scales that correspond to the natural fibrous structure size. The multiscale method can be used to improve the experimental design of natural fiber composite machining and, above all, to determine the optimum process parameters that reflect the multiscale machining characteristics of these ecofriendly materials.

KEYWORDS: (10-15 keywords)

Natural fiber composites; Machining; Surface topography; Surface roughness; Wavelet transform; Analysis of Variance; Surface engineering; Multiscale process signature; Machinability qualification; Analysis scale.

* Corresponding author

1. Introduction

The machining behavior of natural fiber composites (NFC) was presented and discussed in Chapter 7.8. it has been demonstrated that the cutting behavior of natural fibers inside the composite is highly sensitive to the variation of material and process parameters (Chegdani et al., 2016; F. Chegdani et al., 2015; Faissal Chegdani et al., 2015; Chegdani and Mansori, 2018). Indeed, the machining mechanisms of NFC are more complex because natural fibers are themselves a composite material made of cellulose microfibrils embedded in natural polymers of hemicellulose and pectin (Baley, 2002; Charlet et al., 2007). Thus, the heterogeneity is even present inside each elementary fiber. Moreover, natural fibers are gathered in a bundle of dozen of elementary fibers which have random geometries and diameters (Hossain et al., 2013; Morvan et al., 2003). Therefore, NFRP composites exhibit a multiscale heterogeneous structure from elementary fibers (microscale), then fiber bundles (mesoscale) and finally the overall macroscopic composite material (Bos et al., 2004). Exploring the performances of NFC materials has required a multiscale method either for manufacturing process investigation (Doumbia et al., 2015) or for material characterization (Marrot et al., 2014).

For machining processes of NFC parts, a multiscale analysis is also necessary because the mechanical properties of NFC are scale dependent (Chegdani et al., 2017a, 2018c). The standard approaches for the machinability analysis of NFC are not continuously effective to discriminate the effect of some material or process parameters (Chegdani and El Mansori, 2019). In this chapter, these machinability analysis issues are discussed, and a multiscale approach is proposed to substitute the standard methods for the machinability analysis of NFC.

2. Machinability analysis issues of natural fiber composites

The main issues encountered when analyzing the machinability of NFC are related to the quantification of the surface quality, especially the surface topography of machined surfaces. Indeed, the standard methods for surface topography measurements are not able to discriminate the effects of material/process parameters, even if these effects are revealed on the microscopic observations of the machined surfaces. Figure 1 gives some examples of these analysis issues.

Figure 1(a) presents the roughness gain ratio on the machined surfaces of short natural fiber composites to investigates the effect of fiber type and the feed rate on their machinability (F. Chegdani et al., 2015). It has been shown in this study that bamboo fiber composites provide the best fiber shearing while miscanthus fiber composites suffer from interfaces damages during the cutting process. Sisal fiber composites generates the worst machinability where an important rate of uncut fiber extremities remains on the machined surface in addition to decohesion zones caused by interfaces damages. These findings were reproduced on the topographic signals. However, the quantification of these topographic signals by the standard method shows that there is no significant difference between the machined surfaces of bamboo FC and Miscanthus FC at the considered range of the feed rate (Figure 1(a)).

Figure 1(b) presents the roughness measurements obtained by the standard method on the weft fibers zone (fibers oriented toward the feed direction) for bidirectional flax fiber composites to investigate the effect of the helix angle (H) with the milling process (Chegdani et al., 2016). The microscopic observations have revealed that the weft fibers zones generated random cutting behavior of flax fibers which is dependent on the cutting contact location between the cutting edge and the cross sections of flax fibers. As shown in Figure 1(b), the standard method for the quantification of the

surface roughness at macroscopic scale is not able to discriminate the effect of the helix angle on these machined surfaces.

Moreover, Figure 1(c) presents the surface roughness of machines surfaces obtained by orthogonal cutting process of unidirectional flax fiber composites to investigate the effect of the cutting depth and the cutting speed (Chegdani and Mansori, 2018). The microscopic analysis of the machined surfaces reveals that increasing the cutting depth from 100 µm to 500 µm deteriorates the cutting behavior of flax fibers by lowering their shearing efficiency and increasing the interfaces damages. Increasing the cutting speed from 12 m/min to 80 m/min reduces these machining defects. Nevertheless, the quantification of the machined surfaces roughness with the standard method cannot discriminate the effect of the cutting depth at lox cutting speeds as shown in Figure 1(c).

It can be concluded that the standard methods for the quantification of the surface roughness are note suitable for analyzing the machined surfaces of NFC. The main reason can be related to the contact scale between the NFC and the cutting tool (Faissal Chegdani et al., 2015). Figure 2 illustrate the multiscale aspect of the cutting contact in the case of NFC materials. At macroscale, the contact is between the cutting edge radius and the global composite structure (Figure 2(a)). When zooming on the tool/material contact zone, the contact becomes between the fiber bundles and the cutting edge at mesoscale (Figure 2(b)). A further zoom on the tool/material zone reveals the contact at microscale between the cutting edge and the elementary fiber as shown in Figure 2(c). Therefore, A multiscale method for machined surface characterization should be adopted to analyze the machinability of NFC. The proposed multiscale method is presented and discussed in next sections.

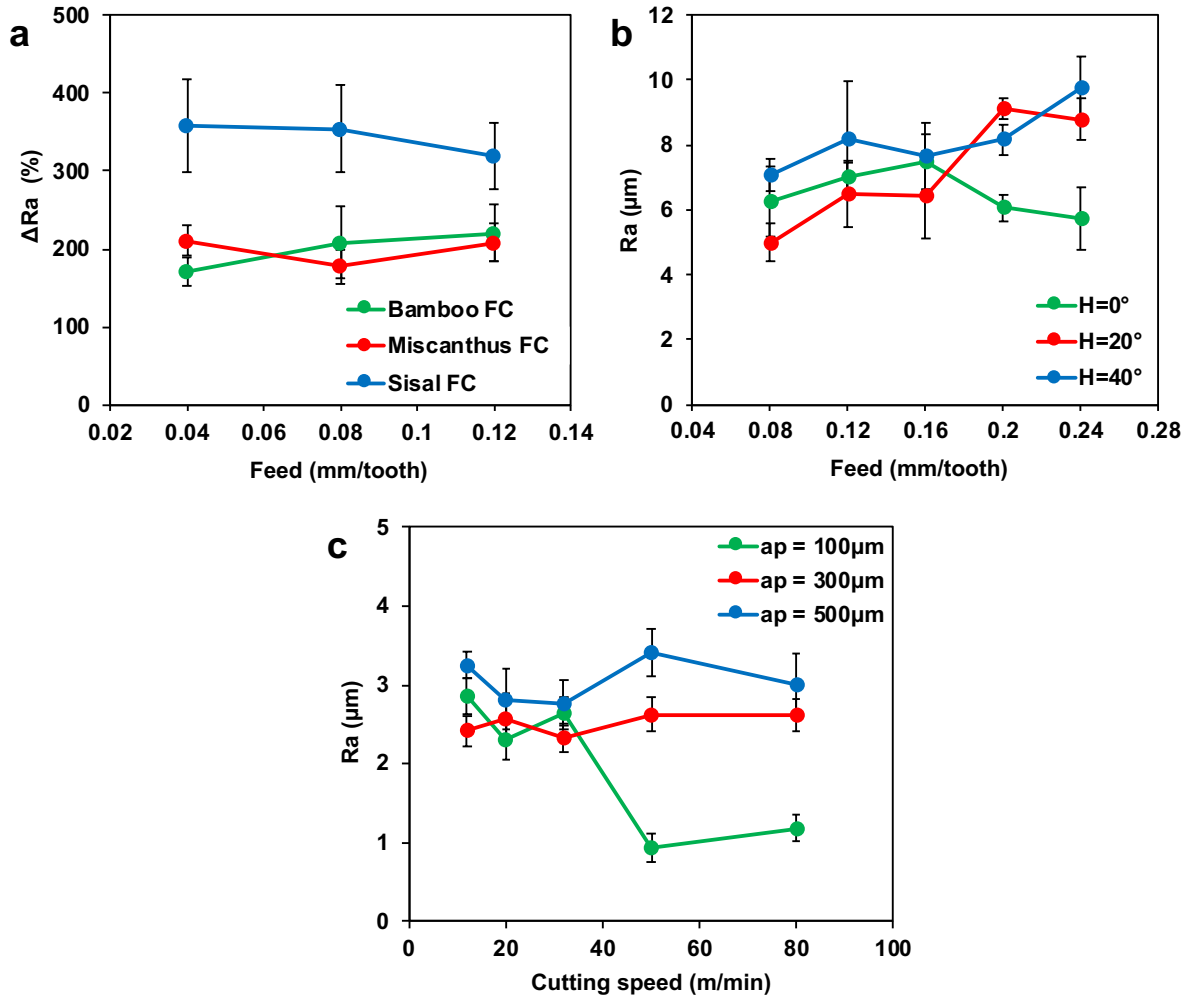

Figure 1: Surface roughness measurements of machined surfaces of NFC from different investigations. (a) Short fiber composites with milling process, (b) Bidirectional flax fiber composites with milling process, and (c) Unidirectional flax fiber composites with orthogonal cutting process.

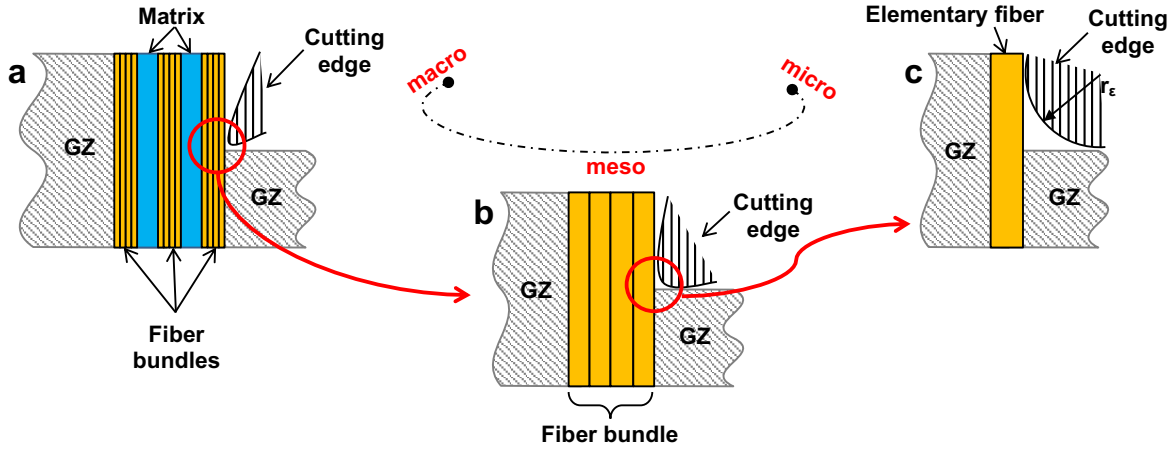

Figure 2: Schematic illustration of the cutting contact scale at (a) macroscale, (b) mesoscale, and (c) microscale. GZ: Global composite zone, r_ε: edge radius

3. Multiscale analysis methodology

The multiscale method is based on a multiscale decomposition of topographic signals using wavelet transform. The idea is to find at which range, each material/process variable affects the morphology of the machined surface. The wavelet transform can be used by discrete wavelet transform (DWT) (Chegdani et al., 2017b) or continuous wavelet transform (CWT) (Chegdani et al., 2016). As described in Figure 3, the aim of this wavelet transform is to decompose the primary topographic signal obtained by the standard method through a series of high-pass and low-pass filters to analyze the high and low frequencies (Chen et al., 2012; Chowdhury et al., 2013; Dick et al., 2012; Katunin, 2011; Peng et al., 2009; Qiu et al., 2016). Since the high frequencies correspond to the micro-roughness and the low frequencies correspond to the waviness, the wavelet transform can quantify the surface morphology at different scale levels.

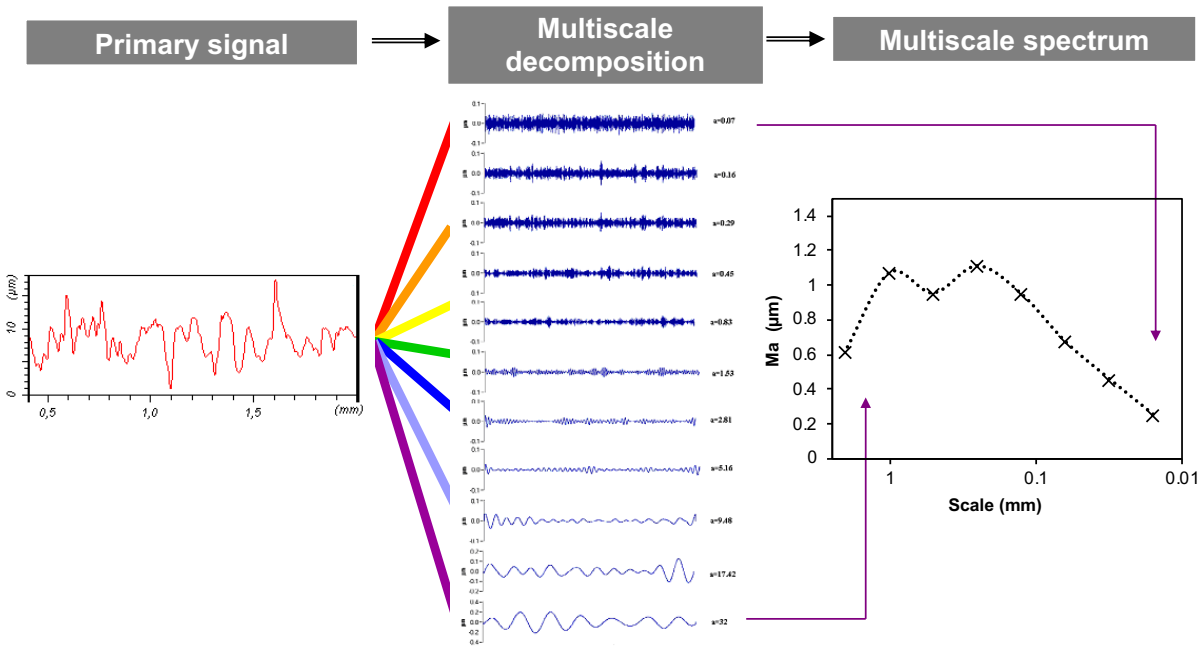

Figure 3: Schematic illustration of the multiscale decomposition method

3.1. Discrete wavelet transform (DWT)

The basic functions to filter the primary topographic signal in DWT are obtained from a single prototype wavelet called the "Mother" wavelet ($\psi(x)$) by translation and dilation (Chen et al., 1995; Daubechies, 1992). The mother wavelet is discretized using the Eq (1) where m and n are, respectively, the translation and dilation parameters. Then, the logarithmic scaling of both dilation and translation steps ($a_0 = 2$ and $b_0 = 1$) generates an orthogonal wavelet shown in Eq (2). The DWT of the global topographic signal (called $f(x)$) is defined by the Eq (3) where $\bar{\psi}_{m,n}(x)$ is the conjugate of the wavelet function. Finally, the reconstruction of the global topographic signal $f(x)$ is given by the Eq (4).

$$\psi_{m,n}(x) = \frac{1}{\sqrt{a_0^m}}\psi\left(\frac{x - nb_0a_0^m}{a_0^m}\right) \quad (1)$$

$$\psi_{m,n}(x) = 2^{-m/2}\psi(2^{-m}x - n) \quad (2)$$

$$W(m,n) = \langle\bar{\psi}_{m,n}(x), f(x)\rangle \quad (3)$$

$$f(x) = \sum_{m,n} W(m,n)\psi_{m,n}(x) \quad (4)$$

3.2. Continuous wavelet transform (CWT)

The continuous wavelet transform of the initial topography signal $f(x)$ is defined by the Eq (5) where $\psi_{a,\vec{b},\theta}(\vec{x}) = \psi_{a,\vec{b}}\left(r_{-\theta}(\vec{x})\right)$ and r_θ is the rotation operator defined by the Eq (6). For 2D continuous wavelet transform, $x = (x,y)$.

In Eq (5), "a" is the contraction coefficient, $\vec{b} = (b_x, b_y)$ the translation coefficient in the x and y directions. Therefore, each component altitude of the global topography signal "f" at the scale "i" in the "(x,y)" point coordinate $f_i(\vec{x},\theta)$ can be thus obtained in each analysis direction "θ" by inverse wavelets transform.

$$W_{\psi}^{f}(a,b,\theta) = \frac{1}{a}\int_{-\infty}^{+\infty}\int_{-\infty}^{+\infty} f(\vec{x})\psi_{a,\vec{b},\theta}^{*}(\vec{x})d\vec{x} \quad (5)$$

$$r_{\theta}(x,y) = (x\,cos\theta + y\,sin\theta - x\,sin\theta + y\,cos\theta) \quad (6)$$

3.3. Multiscale roughness quantification

After the wavelet transform, the arithmetic mean roughness can be quantified at each scale of the decomposition. This multiscale arithmetic mean roughness is called "Ma" for 1D line topographic profiles (x) and "SMa" for 2D surface topographic profiles (x,y). This arithmetic mean value can be obtained using the Eq (7) and Eq (8) where $f_i(x)$ and $f_i(x,y)$ are respectively the component altitude of the global topographic signal at the scale "i" in the point coordinate (x) and (x,y). "N" and "M" represent respectively the number of points in the x and the y directions (Chegdani and El Mansori, 2019).

$$M_a(i) = \sum_{x=1}^{M}\frac{|f_i(x)|}{M} \quad (7)$$

$$SM_a(i) = \sum_{x=1}^{M}\sum_{y=1}^{N}\frac{|f_i(x,y)|}{MN} \quad (8)$$

Finally, the obtained values of Eq (7) or Eq (8) allow the determination of the multiscale process signature (MPS) which is equivalent to a transfer function that can be compared directly with the multiscale modifications of the surface topography. This MPS depicts the signatures of the finishing process in terms of essential changes of the surface state produced on the original surface (El Mansori et al., 2010). The MPS is defined at each scale "i" by Eq (9) and Eq (10) for 1D line topographic profiles and 2D surface topographic profiles, respectively. In these two equations, "F" and "I" refer to final state and the initial state of the machined surfaces, respectively.

$$MPS(i) = \frac{M_a^F(i) - M_a^I(i)}{M_a^I(i)} \times 100 \quad (9)$$

$$MPS(i) = \frac{SM_a^F(i) - SM_a^I(i)}{SM_a^I(i)} \times 100 \quad (10)$$

After filtering the pertinent scales by the MPS, the mean process signature (ΔMPS) can be calculated to assess the morphology modifications due to the machining process without the parasitic effects of the impertinent scales. ΔMPS is defined by Eq (11) where "P" is the number of the pertinent scales in the wavelet decomposition.

$$\Delta MPS = \sum_{i=1}^{P} \frac{MPS(i)}{P} \quad (11)$$

4. Machinability analysis of natural fiber composites with the multiscale methodology

4.1. Scale effect on the machined surface roughness

The machining analysis issues presented in section 2 have been handled by the multiscale method described in section 3. Each primary signal obtained by the standard methods has been processed using either the DWT or the CWT.

Figure 4(a) shows the multiscale spectrum obtained from the primary signals of the machined surface of short fiber composites investigated in (F. Chegdani et al., 2015). The scale effect of the topographic response of the machines surfaces is clearly obvious. The roughness is at its lowest values at microscale and increases by increasing the analysis scale until reaching a macroscale of 1 mm. The roughness decreases after exceeding this macroscale value.

Figure 4(a) show also that the effect of fiber type is clearly discriminated at the scale range between 0.1 mm and 0.5 mm. this mesoscale range correspond to the size of

the fiber bundles used in the short fiber composites materials. Therefore, the relevant scale of the machinability analysis of NFC is related to the mesoscale of the natural fibrous reinforcement.

By considering only the mesoscale for the analysis of the machined surface roughness, Figure 4(b) reveals that the effects of fiber type and cutting feed are obviously distinguished where increasing the cutting feed decreases the surface roughness. Moreover, Bamboo fibers, that have the highest rigidity, generate the lowest surface roughness while sisal fibers, that have the lowest rigidity, generate the highest surface roughness. These findings shown in Figure 4(b) are not provided on the results of the standard analysis methods presented in Figure 1(a) where the effect of fiber type is not differentiated between bamboo and miscanthus fibers.

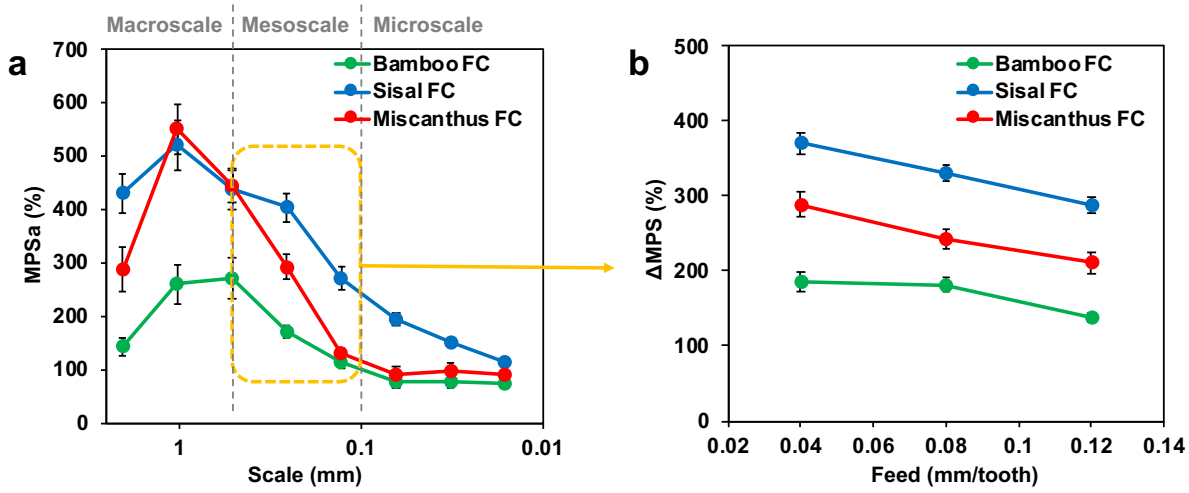

Figure 4: (a) Multiscale process signature on machined surfaces of short fiber composites obtained by discrete wavelet transform. (b) Process signature at mesoscale on machined surfaces of short fiber composites.

Figure 5(a) shows the multiscale spectrum obtained from the primary signals of the machined surface of bidirectional flax fiber composites investigated in (Chegdani et al., 2016). The spectrums in Figure 5(a) were obtained as the mean of 20 topographic profiles extracted from both warp fiber zones and weft fiber zones in order to generate a representative output for all the machined surface.

It can be seen from Figure 5(a) that the effect of tool helix angle is revealed at the scale range between 0.1 mm and 1 mm. This scale range matches to the flax reinforcement structure size used in the considered composite because 0.1 mm corresponds approximately to the diameter of the technical fiber and 1 mm corresponds approximately to the diameter of the flax yarns formed by the technical fibers.

Figure 5(b) shows the multiscale spectrum obtained from the primary signals of the machined surface of unidirectional flax fiber composites investigated in (Chegdani and Mansori, 2018) with a cutting speed of 20 m/min. In this multiscale study, the analysis scale affects also the roughness response that increases by increasing the analysis scale. As for the case of bidirectional flax fiber composites (Figure 5(a)), the effect of cutting depth is revealed at the scale range between 0.1 mm and 1 mm which correspond to the flax reinforcement structure size.

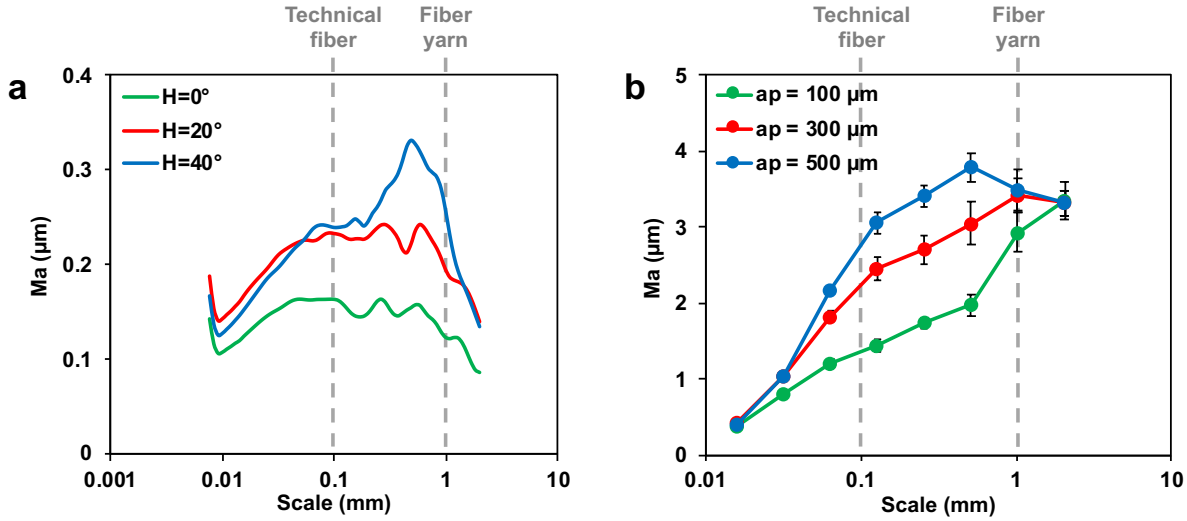

Figure 5: (a) Multiscale process signature on machined surfaces of bidirectional flax fiber composites obtained by continuous wavelet transform. (b) Multiscale process signature on machined surfaces of unidirectional flax fiber composites obtained by discrete wavelet transform.

4.2. Multiscale contribution of machining parameters on the surface roughness

To quantify the effect of source factors on the roughness level at each scale of the decomposition, mathematical models for machining of NFC using regression analysis and the analysis of variance (ANOVA) (Davim and Reis, 2005; Gonsalez et al., 2015) were elaborated. Linear regression analysis for the results of the multiscale surface roughness analysis was considered.

Sequential approach or Type I sum of squares was used to test main effects and interaction behaviors in ANOVA. It allows, first, to allocate the part of the explained variance to the main effects (one after the other), then to the two-way interaction(s) (one after the other) and then to increasingly higher-order interactions if present (Kherad-Pajouh and Renaud, 2010).

Experimental and predicted multiscale surface roughness responses are compared. The sum of squares (SS) and the fitted residual sum of squares (RSS) of these gaps are computed and collected from all the parallel models to form the predictive residual sum of squares ($PRESS$) which estimates the predictive ability of the model. The goodness-of-fit is evaluated for the considered model with the measure of the squared correlation coefficient (R^2) and the cross-validated squared correlation coefficient (Q^2) (Wold et al., 2001). Where:

$$R^2 = 1 - \frac{RSS}{SS} \tag{12}$$

$$Q^2 = 1 - \frac{PRESS}{SS} \tag{13}$$

R^2 is a real number between zero and one. A large value of R^2 indicates a better fitness of the model to the data. The predictive capability of a model is generally determined by Q^2 which is usually between zero and one. A higher Q^2 value indicates a more

reliable model with excellent predictive power (Wang et al., 2013). Q^2 can be negative for very poor models.

After the validation of the model with R^2 and Q^2, *F*-test (Massart et al., 1998) was used to quantify the significance of each input working factor "α" by Eq (14) where MS_{reg} is the mean square due to regression and MS_r is the residual mean square.

$$F(\alpha) = \frac{MS_{reg}(\alpha)}{MS_r} \tag{14}$$

To quantify the contribution of the studied material/process parameters, ANOVA of input variables influence has been performed at each multiscale response of surface quality (i.e. at each scale "α" of the decomposition) using XLSTAT software. The contribution ratio of each "α" factor (C_α) was calculated with the Fisher criterion test ($F(\alpha)$) at the correlation coefficient (R^2) confidence (Davim and Reis, 2005; Massart et al., 1998). Eq (15) defines the contribution ratio of each factor.

$$C_\alpha = \frac{F(\alpha)}{\sum_\alpha F(\alpha)} \times R^2 \tag{15}$$

The ANOVA analysis was applied to the multiscale roughness data shown in Figure 4(a) where the contribution rates of fiber type and cutting feed were determined (Chegdani et al., 2017b). Figure 6(a) reveals that the contribution rates of natural fiber stiffness and feed factors are different at each analysis scale and present specific behaviors at three characteristic zones that are closed to the characteristic zones defined by multiscale surface roughness analysis of Figure 4(a). At microscale, fiber stiffness contribution increases significantly by scale increasing while feed contribution decreases significantly until becoming negligible. Interaction contribution is insignificant in this zone and also at mesoscale. This mesoscale area reveals an opposite behavior comparing to the microscopic zone where fiber stiffness contribution decreases significantly by scale increasing while feed contribution increases by scale

increasing. This trend is spread until the scale a = 1mm that shows the most significant contribution of the interactions between fiber stiffness and feed effects. Feed effect reaches its maximum and fiber stiffness effect reaches its minimum. At macroscale, fiber stiffness contribution re-increases by scale increasing while feed contribution re-decreases by scale increasing. This multiscale behavior of the contribution rates of material/process parameters is intrinsically related to the multiscale structure of the NFC materials (Chegdani et al., 2017b).

The ANOVA analysis was also applied to the multiscale roughness data shown in Figure 5(b) in order to determine the contributions of cutting depth, cutting speed and edge radius (Chegdani and Mansori, 2018). Figure 6(b) presents the contribution rate of each process parameter at each analysis scale. It can be seen the low contribution of the cutting edge radius regarding the other parameters until the macroscale. The behavior of the multiscale contribution rates confirms the previous results shown in Figure 5(b). Indeed, Figure 6(b) shows the significant impact of the cutting depth at the relevant scale identified in Figure 5(b). At macroscopic scale, the random distribution of technical fibers influences the contribution of the process parameters and increases the contribution of the interactions (Chegdani and Mansori, 2018).

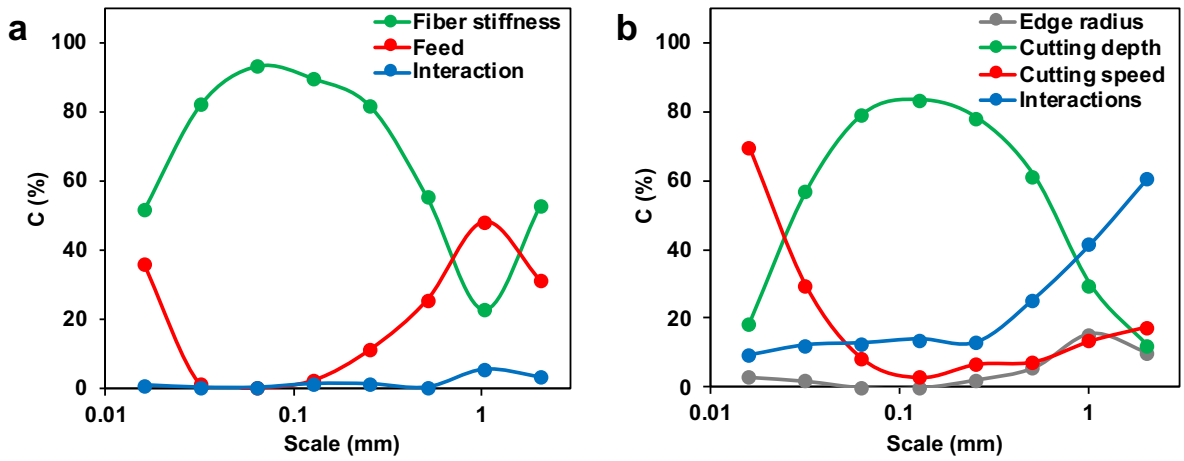

Figure 6: contribution rate of process parameters for (a) milled surfaces of short fiber composites, and (b) machined surfaces of unidirectional flax fiber composites with orthogonal cutting process

5. New multiscale approach for the machinability analysis of natural fiber composites

5.1. Principle of the new multiscale approach

Based on the results presented in section 4, machining qualification of natural fiber composites requires the selection of the relevant scale for the cutting process analysis. The pertinent scale corresponds to the size of the fibrous structure regardless of the reinforcement structure type (Chegdani and El Mansori, 2019). This specific analysis allows an efficient discrimination of the effects of material/process parameters.

Concretely, Figure 7 illustrates the principle of the new multiscale approach that should be applied for the analysis of the machinability of NFC materials. Indeed, to qualify effectively the machinability of the NFC parts, the natural fibrous structure should be first analyzed in order to determine the fibrous structure size. The value of the fibrous structure size will correspond then to the relevant analysis scale on which the topographic analysis of the machined surfaces of NFC parts should be performed to evaluate their machinability.

The relationship between the relevant scale and the fibrous structure size has been previously confirmed by nanoindentation and scratch test measurements that show the scale effect on the tribo-mechanical performances of flax fibers (Chegdani et al., 2017a, 2018c). Unlike glass fibers that have a homogeneous mechanical behavior, the tribo-mechanical response of flax fibers induces a multiscale behavior that depends on the mechanical contact scale. This reveals the specificity when cutting natural fibers and the importance of considering the analysis scale for robust machining analysis of NFC materials in industrial applications.

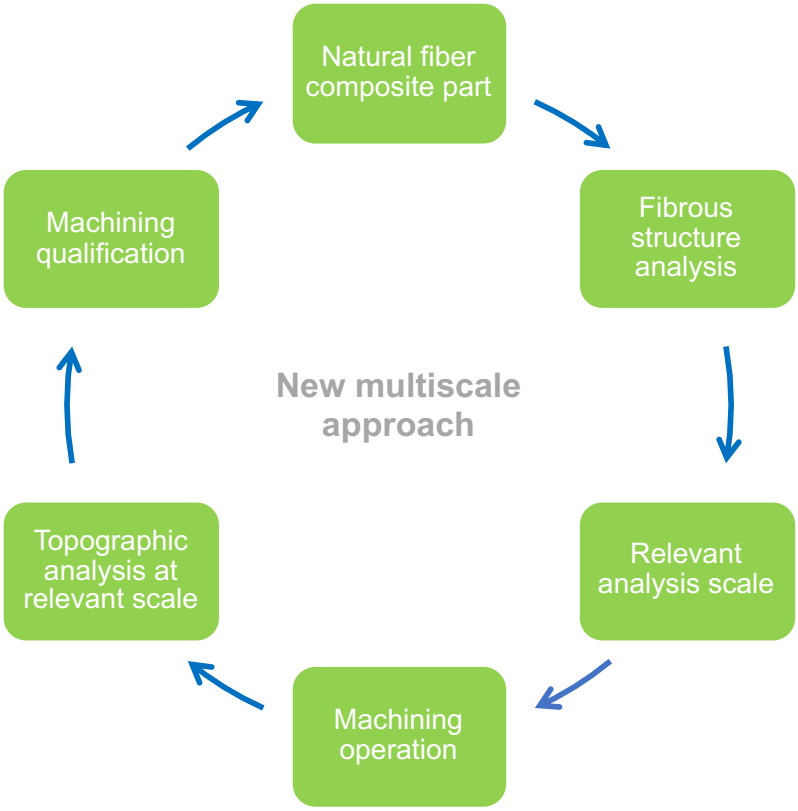

Figure 7: Principle of the multiscale approach for machinability analysis of natural fiber composites

5.2. Validation of the new multiscale approach

The validation of the new multiscale approach for machinability analysis of NFC has been performed on an industrial part provided by Faurecia Automotive Industry (Chegdani and El Mansori, 2019). The industrial NFC is a sandwich part as shown in Figure 8(a). The skins are composite plates molded of unidirectional flax fibers and Acrodur bio-resin. The honeycomb structure is made of cardboard. Each skin of the sandwich NFC consists of three layers of unidirectional long flax fibers bonded by the Acrodur resin. The density of the fibers in each layer is about 200 g/m². This gives the skin a thickness of 1 mm. The three layers of UD flax/Acrodur in each skin have a fiber orientation configuration of 0°/90°/0°. This fibrous reinforcement structure will generate warp fiber zone (WPZ) and weft fiber zone (WTZ) as for the case of bidirectional flax

fiber composites investigated in section 2 and section 4. The thickness of the cardboard honeycomb structure is 20 mm.

As suggested by the new multiscale approach, the fibrous reinforcement is analyzed with SEM observation as shown in Figure 8(b). It can be seen that the fibrous structure is in form of non-twisted technical flax fibers that have diameter values between 150 µm and 200 µm.

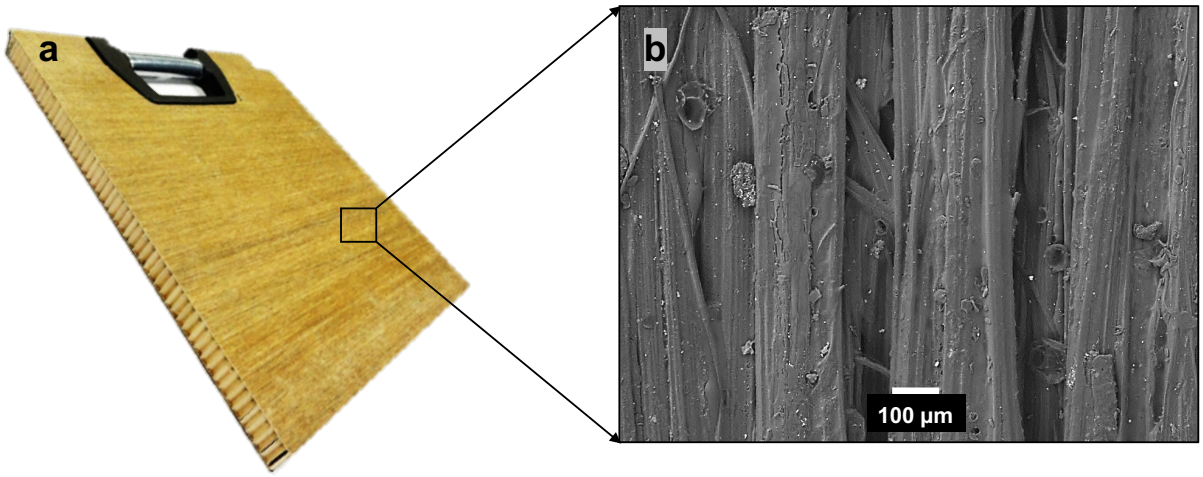

Figure 8: (a) Image of the industrial sandwich part. (a) SEM image of the flax fibrous reinforcement in the sandwich skins

Milling process is considered to perform the machining experiments on the sandwich part. The analysis focuses on the profile surface state of the sandwich skin (UD flax and Acrodur resin). The behavior of the cardboard honeycomb structure is not considered. The effect of cutting speed and cutting feed is investigated in this study. The topographic analysis of the machined surfaces of the sandwich skins are realized with respect to the recommendations of the multiscale approach. Indeed, the optical objective of the interferometer has been chosen and adjusted to produce topographic image dimensions that correspond to the scale of the technical fibers size (~ 150 – 200 µm).

Figure 9(a) present a typical topographic image of the machined surfaces at the relevant scale that allows to cover the two fiber zones (WPZ and WTZ). The resulting

arithmetic mean roughness of the machined surfaces at the relevant scale are presented in Figure 9(b). Unlike the standard topographic analysis on bidirectional flax fiber composites that shows a random behavior of the surface roughness results (Figure 1(b)), the topographic analysis performed in accordance with the new multiscale approach allow to get a pertinent evaluation of the effect of both the cutting speed and the cutting feed as shown in Figure 9(b). Overall, the surface roughness increases by increasing the feed rate and decreases by increasing the cutting speed. The multiscale analysis approach leads to find an optimum of cutting speed and feed rate for machining the industrial sandwich part. The roughness is at its lowest value for feed rate of 0.04 mm/tooth and for a cutting speed of 300 m/min. Consequently, these cutting conditions are the best-suited parameters for this material to guarantee the smoothest surfaces after machining with fewer surface damages.

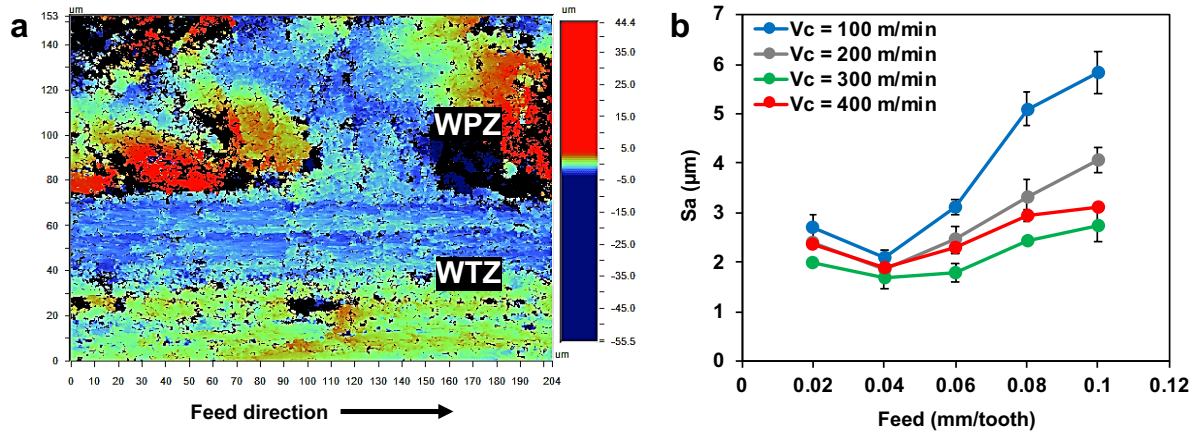

Figure 9: (a) topographic image at the relevant scale on the machined surface of the sandwich skin. (b) Arithmetic mean surface roughness of the machined surface of the sandwich skin performed at the relevant scale.

The new multiscale approach has also been validated during the investigation of the surface forming of unidirectional flax fibers reinforced polypropylene composites using the mechanical polishing process at dry and wet polishing conditions (Chegdani et al., 2018a). As shown in section 4.1 and Figure 5(b), the relevant scale for this kind of NFC is in the scale range between 0.1 mm and 1 mm which correspond to the flax reinforcement structure size. Therefore, the topographic analysis of the polished

surfaces has been performed using an optical objective of the interferometer that generates a topographic image size of 840×840 μm^2 as shown in Figure 10(a). The resulting arithmetic mean roughness of the polished surfaces at the relevant scale are presented in Figure 10(b). The roughness calculation at the relevant scale allows a good discrimination of the effect of each polishing configuration. Indeed, wet polishing induces more surface roughness than dry polishing because of the fracture of the interfaces caused by water lubrication (Chegdani et al., 2018a). These interface fractures are more intense when polishing with high grit size (GS in Figure 10(b)) which further increases the surface roughness of the wet polished surfaces comparing to the dry polished surfaces.

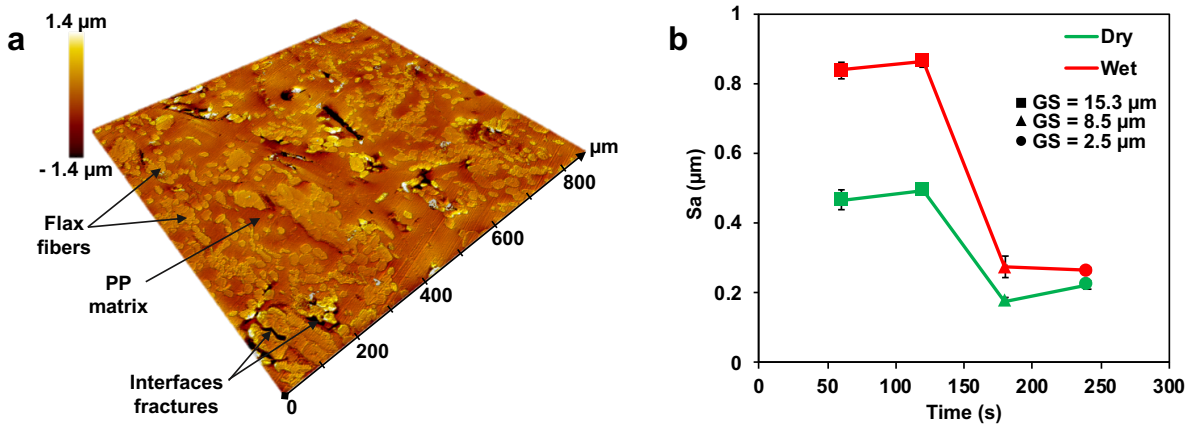

Figure 10: (a) typical topographic image of the polished surfaces of unidirectional flax fiber composites at the relevant scale. (b) Arithmetic mean surface roughness of the polished surfaces of unidirectional flax fiber composites at the relevant scale

The same unidirectional flax fiber composites have been used in other study to investigate the effects of sample temperature and rake angle on the machining behavior of the NFC using the orthogonal cutting process (Chegdani et al., 2018b). As for the investigation of the polishing process, the topographic analysis of the machined surfaces is performed using an optical objective of the interferometer that generates a topographic image size of 840×840 μm^2 as shown in Figure 11(a). The resulting arithmetic mean roughness of the machined surfaces at the relevant scale are

presented in Figure 11(b). It can be seen once again that the roughness calculation at the relevant scale allows a good discrimination of the effect of sample temperature and rake angle for the orthogonal cutting process of unidirectional flax fiber composites. Lowering the sample temperature leads to decrease the machined surface roughness by increasing the rigidity of flax fibers and polymer matrix (Chegdani et al., 2018b). This investigation with the new multiscale approach suggests also to perform the cutting operation with positive rake angle to increase the cutting contact stiffness and then reduce machined surface roughness as shown in Figure 11(b).

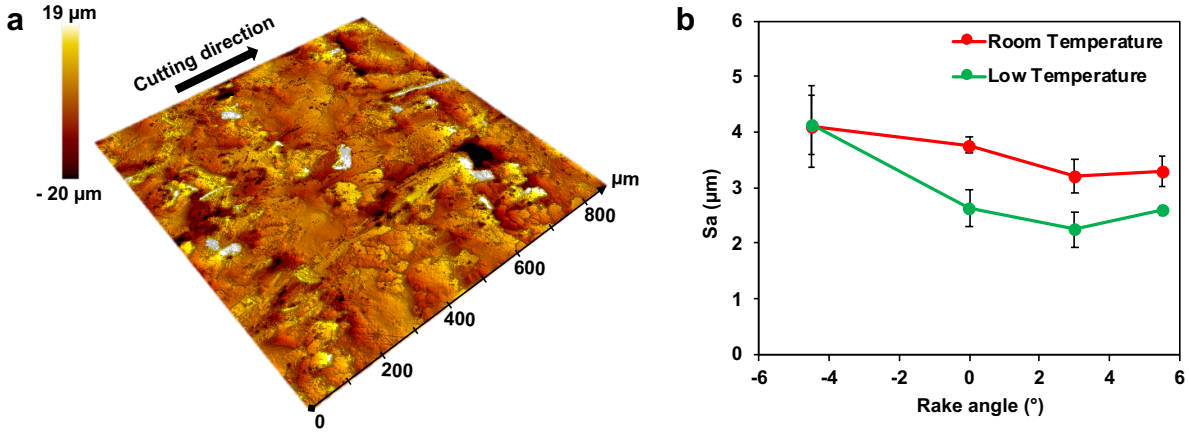

Figure 11: (a) typical topographic image of the machined surfaces of unidirectional flax fiber composites at the relevant scale. (b) Arithmetic mean surface roughness of the machined surfaces of unidirectional flax fiber composites at the relevant scale

6. Conclusions

Machining of natural fiber composites encounters some issued related to the machinability analysis. Indeed, the qualification of the machinability of natural fiber composites is complicated with the standard approach, especially for the quantification of the machined surfaces because of the complex multiscale structure of natural fiber composites. In this study, these machinability analysis issues are presented and discussed. Moreover, a new multiscale approach is developed and proposed to

address the machinability qualification of natural fiber composites. The main following conclusions can be drawn:

- Regardless of the natural reinforcement structure types, the relevant scale for analyzing the machined surfaces of natural fiber composites are the scale that corresponds to the fibrous structure size.
- Unlike the standard approaches for the quantification of the machined surface roughness, the new multiscale approach recommends analyzing first the natural fibrous structure and determine its size. The fibrous structure size value should correspond to the pertinent scale on which the topographic analysis of machined surfaces should be performed. This will allow an efficient discrimination of the material/process effects on the surface quality of natural fiber composites.
- The new multiscale approach has been validated on different machining investigations and has shown its strength to provide an appropriate machinability qualification of natural fiber composites.

7. References

Baley, C., 2002. Analysis of the flax fibres tensile behaviour and analysis of the tensile stiffness increase. Compos. - Part A Appl. Sci. Manuf. 33, 939–948. https://doi.org/10.1016/S1359-835X(02)00040-4

Bos, H.L., Molenveld, K., Teunissen, W., van Wingerde, A.M., van Delft, D.R. V, 2004. Compressive behaviour of unidirectional flax fibre reinforced composites. J. Mater. Sci. 39, 2159–2168. https://doi.org/10.1023/B:JMSC.0000017779.08041.49

Charlet, K., Baley, C., Morvan, C., Jernot, J.P., Gomina, M., Bréard, J., 2007. Characteristics of Hermès flax fibres as a function of their location in the stem

and properties of the derived unidirectional composites. Compos. Part A Appl. Sci. Manuf. 38, 1912–1921. https://doi.org/10.1016/j.compositesa.2007.03.006

Chegdani, F., Bukkapatnam, S.T.S., Mansori, M. El, 2018a. Thermo-mechanical Effects in Mechanical Polishing of Natural Fiber Composites. Procedia Manuf. 26, 294–304. https://doi.org/10.1016/j.promfg.2018.07.038

Chegdani, F., El Mansori, M., 2019. New Multiscale Approach for Machining Analysis of Natural Fiber Reinforced Bio-Composites. J. Manuf. Sci. Eng. Trans. ASME 141, 11004. https://doi.org/10.1115/1.4041326

Chegdani, F., El Mansori, M., Mezghani, S., Montagne, A., 2017a. Scale effect on tribo-mechanical behavior of vegetal fibers in reinforced bio-composite materials. Compos. Sci. Technol. 150, 87–94. https://doi.org/10.1016/j.compscitech.2017.07.012

Chegdani, F., Mansori, M. El, 2018. Mechanics of material removal when cutting natural fiber reinforced thermoplastic composites. Polym. Test. 67, 275–283. https://doi.org/10.1016/j.polymertesting.2018.03.016

Chegdani, F., Mezghani, S., El Mansori, M., 2017b. Correlation between mechanical scales and analysis scales of topographic signals under milling process of natural fibre composites. J. Compos. Mater. 51, 2743–2756. https://doi.org/10.1177/0021998316676625

Chegdani, F., Mezghani, S., El Mansori, M., 2016. On the multiscale tribological signatures of the tool helix angle in profile milling of woven flax fiber composites. Tribol. Int. 100, 132–140. https://doi.org/10.1016/j.triboint.2015.12.014

Chegdani, Faissal, Mezghani, S., El Mansori, M., 2015. Experimental study of coated tools effects in dry cutting of natural fiber reinforced plastics. Surf. Coatings Technol. 284, 264–272. https://doi.org/10.1016/j.surfcoat.2015.06.083

Chegdani, F., Mezghani, S., El Mansori, M., Mkaddem, A., 2015. Fiber type effect on tribological behavior when cutting natural fiber reinforced plastics. Wear 332–333, 772–779. https://doi.org/10.1016/j.wear.2014.12.039

Chegdani, F., Takabi, B., Tai, B.L., Mansori, M. El, Bukkapatnam, S.T.S., 2018b. Thermal Effects on Tribological Behavior in Machining Natural Fiber Composites. Procedia Manuf. 26, 305–316. https://doi.org/10.1016/j.promfg.2018.07.039

Chegdani, F., Wang, Z., El Mansori, M., Bukkapatnam, S.T.S., 2018c. Multiscale tribo-mechanical analysis of natural fiber composites for manufacturing applications. Tribol. Int. 122, 143–150. https://doi.org/10.1016/j.triboint.2018.02.030

Chen, B., Zhang, Z., Sun, C., Li, B., Zi, Y., He, Z., 2012. Fault feature extraction of gearbox by using overcomplete rational dilation discrete wavelet transform on signals measured from vibration sensors. Mech. Syst. Signal Process. 33, 275–298. https://doi.org/10.1016/j.ymssp.2012.07.007

Chen, X., Raja, J., Simanapalli, S., 1995. Multi-scale analysis of engineering surfaces. Int. J. Mach. Tools Manuf. 35, 231–238. https://doi.org/10.1016/0890-6955(94)P2377-R

Chowdhury, S.K., Nimbarte, A.D., Jaridi, M., Creese, R.C., 2013. Discrete wavelet transform analysis of surface electromyography for the fatigue assessment of neck and shoulder muscles. J. Electromyogr. Kinesiol. 23, 995–1003. https://doi.org/10.1016/j.jelekin.2013.05.001

Daubechies, I., 1992. Ten Lectures on Wavelets, Society for Industrial and Applied Mathematics “SIAM.” Philadelphia. https://doi.org/10.1137/1.9781611970104

Davim, J.P., Reis, P., 2005. Damage and dimensional precision on milling carbon

fiber-reinforced plastics using design experiments. J. Mater. Process. Technol. 160, 160–167. https://doi.org/10.1016/j.jmatprotec.2004.06.003

Dick, A.J., Phan, Q.M., Foley, J.R., Spanos, P.D., 2012. Calculating scaling function coefficients from system response data for new discrete wavelet families. Mech. Syst. Signal Process. 27, 362–369. https://doi.org/10.1016/j.ymssp.2011.09.015

Doumbia, A.S., Castro, M., Jouannet, D., Kervoëlen, A., Falher, T., Cauret, L., Bourmaud, A., 2015. Flax/polypropylene composites for lightened structures: Multiscale analysis of process and fibre parameters. Mater. Des. 87, 331–341. https://doi.org/10.1016/J.MATDES.2015.07.139

El Mansori, M., Mezghani, S., Sabri, L., Zahouani, H., 2010. On concept of process signature in analysis of multistage surface formation. Surf. Eng. 26, 216–223. https://doi.org/10.1179/174329409X455412

Gonsalez, C.G., da Silva, S., Brennan, M.J., Lopes Junior, V., 2015. Structural damage detection in an aeronautical panel using analysis of variance. Mech. Syst. Signal Process. 52–53, 206–216. https://doi.org/10.1016/j.ymssp.2014.04.015

Hossain, R., Islam, A., Vuure, A. Van, Verpoest, I., 2013. Processing dependent flexural strength variation of jute fiber reinforced epoxy composites. J. Eng. Appl. Sci. 8, 513–518.

Katunin, A., 2011. Damage identification in composite plates using two-dimensional B-spline wavelets. Mech. Syst. Signal Process. 25, 3153–3167. https://doi.org/10.1016/j.ymssp.2011.05.015

Kherad-Pajouh, S., Renaud, O., 2010. An exact permutation method for testing any effect in balanced and unbalanced fixed effect ANOVA. Comput. Stat. Data Anal. 54, 1881–1893. https://doi.org/10.1016/j.csda.2010.02.015

Marrot, L., Bourmaud, A., Bono, P., Baley, C., 2014. Multi-scale study of the adhesion between flax fibers and biobased thermoset matrices. Mater. Des. 62, 47–56. https://doi.org/10.1016/J.MATDES.2014.04.087

Massart, D.L., Vandeginste, B.G.M., Buydens, L.M.C., De Jong, S., Lewi, P.J., Smeyers-Verbeke, J., 1998. Handbook of Chemometrics and Qualimetrics: Part A, Data Handl. ed. Elsevier B.V., Amsterdam.

Morvan, C., Andème-Onzighi, C., Girault, R., Himmelsbach, D.S., Driouich, A., Akin, D.E., 2003. Building flax fibres: more than one brick in the walls. Plant Physiol. Biochem. 41, 935–944. https://doi.org/10.1016/j.plaphy.2003.07.001

Peng, Z.K., Jackson, M.R., Rongong, J.A., Chu, F.L., Parkin, R.M., 2009. On the energy leakage of discrete wavelet transform. Mech. Syst. Signal Process. 23, 330–343. https://doi.org/10.1016/j.ymssp.2008.05.014

Qiu, Z., Lee, C.-M., Xu, Z.H., Sui, L.N., 2016. A multi-resolution filtered-x LMS algorithm based on discrete wavelet transform for active noise control. Mech. Syst. Signal Process. 66–67, 458–469. https://doi.org/10.1016/j.ymssp.2015.05.024

Wang, H., Shangguan, L., Wu, J., Guan, R., 2013. Multiple linear regression modeling for compositional data. Neurocomputing 122, 490–500. https://doi.org/10.1016/j.neucom.2013.05.025

Wold, S., Sjöström, M., Eriksson, L., 2001. PLS-regression: a basic tool of chemometrics. Chemom. Intell. Lab. Syst. 58, 109–130. https://doi.org/10.1016/S0169-7439(01)00155-1